Proceedings of the VI Hispalensis International Summer School

Many-Body Theory of Correlated Fermion Systems

Oromana, Sevilla, Spain June 9–21 1997

Editors

José M. Arias,
M. Isabel Gallardo
Manuel Lozano
University of Sevilla, Spain

World Scientific
Singapore • New Jersey • London • Hong Kong

Published by

World Scientific Publishing Co. Pte. Ltd.

P O Box 128, Farrer Road, Singapore 912805

USA office: Suite 1B, 1060 Main Street, River Edge, NJ 07661

UK office: 57 Shelton Street, Covent Garden, London WC2H 9HE

British Library Cataloguing-in-Publication Data
A catalogue record for this book is available from the British Library.

MANY-BODY THEORY OF CORRELATED FERMION SYSTEMS

ISBN 981-02-3383-3

This book is printed on acid-free paper.

Printed in Singapore by Uto-Print

A MICROSCOPIC THEORY OF MAGNETIC ORDER IN STRONGLY CORRELATED QUANTUM SPIN LATTICES

R.F. BISHOP and D.J.J. FARNELL
Department of Physics, UMIST
(University of Manchester Institute of Science and Technology)
P.O. Box 88, Manchester M60 1QD, UK

Quantum spins arranged on regular geometrical lattices, and interacting through a wide diversity of specified model Hamiltonians, provide a rich variety of magnetically ordered phases with many subtle properties. The zero-temperature quantum phase transitions between states of different order can be explored by the variation of internal control parameters within the interaction Hamiltonian. We illustrate how the systematic inclusion of multi-spin correlations for such lattice systems may be efficiently and effectively implemented via the coupled cluster method (CCM), which has been widely demonstrated on many previous occasions to be one of the most versatile methods of microscopic quantum many-body theory. Its power is illustrated by application to the spin-$\frac{1}{2}$ anisotropic Heisenberg (or XXZ) model on an infinite square lattice. The results obtained for such properties as the ground-state energy and sublattice magnetization are found to be as accurate as those obtained by any available alternative method. We show also how the CCM can now provide accurate *ab initio* estimates for the critical values of the parameters which mark the positions of phase boundaries between states of different quantum order, as well as for the critical indices associated with the singular behaviour near these transition points of various physical quantities.

1 Introduction

There has been a continuing refinement over the last ten years of the fundamental techniques of microscopic quantum many-body theory. This development is particularly striking for what is nowadays recognized as providing perhaps the most powerful, most widely applicable, and most accurate at attainable levels of practical implementation, of all available *ab initio* techniques, namely the coupled cluster method (CCM) [1-9]. Results obtained by the use of the CCM have become fully competitive, for example, with series expansions, variational calculations, and even quantum Monte Carlo simulations for those cases in which this latter method may be applied.

However, despite the many achievements of the CCM and other techniques of modern quantum many-body theory, their use has been largely limited up till now to a local description of the properties of the system under consideration, rather than to its global behaviour. Thus, until very recently, most of these fully microscopic calculations had been restricted to calculations of such local properties as the ground-state energy, the excitation spectrum, and such

other properties as the relevant order parameters and correlation functions. By contrast, very little progress had been made on using the *same* techniques to make contact at the microscopic level with the otherwise quite disparate corpus of work which relates to the study of phase transitions in infinite systems and to related (e.g., shape) transitions in finite systems. This situation is now beginning to change in fundamental ways, due largely to recent results obtained using the CCM which we describe here.

At a rather general level there are now many physical systems which are characterized by novel ground states which display *quantum order* in some regions of the relevant parameter space. Such regions are delimited by critical values which mark the respective *quantum phase transitions*. Very often, the critical phenomena displayed by the quantum systems differ profoundly from their corresponding classical counterparts (where they exist). The subtly correlated quantum-mechanical states usually cannot sensibly be viewed within the traditional language of Landau's theory of Fermi liquids, for example, or of other comparable phenomenological approaches which have been so useful in the past for so many conventional quantum many-body systems. Examples of systems or phenomena which fall into the unconventional (or novel) class include heavy fermions, the fractional quantum Hall effect, new quantum states in the condensed phases of helium, confinement/deconfinement phase transitions in gauge field theories, high-temperature superconductors and other strongly correlated electronic systems, and various phases of (antiferro)magnetic materials and low-dimensional quantum spin lattices.

Standard many-body techniques, such as perturbation theory, mean-field theories, and variational calculations, which have successfully treated conventional systems, typically fail completely for these unconventional systems characterized by novel quantum order. A key challenge for modern quantum many-body theory is now to develop and exploit microscopic techniques which are capable of describing both these novel and the more conventional systems. A prime objective of our own work on quantum lattice systems [10-18] has been to show that at least one such modern technique, namely the CCM, is in fact already able to bridge these two classes of systems.

The CCM has been applied over the last five or so years to many lattice Hamiltonian systems [15,16], including spin lattices of interest, for example, in magnetism [10-14, 19-26] and the solid phases of ^{3}He [19]; electron lattice models of interest, for example, in the cuprate high-temperature superconductors (e.g., the Hubbard model) [17,27]; and lattice gauge theories, such as the Abelian $U(1)$ model [18] and the non-Abelian $SU(2)$ model [28]. In all cases the CCM may be implemented to high orders of approximation by the use of computer-algebraic techniques. Values for ground-state (and, increasingly, also

excited-state) properties are thereby obtained which are fully competitive with those from other state-of-the-art calculations, including the much more computationally intensive quantum Monte Carlo techniques. What we now further demonstrate, by a specific application to the spin-$\frac{1}{2}$ anisotropic Heisenberg model on the two-dimensional (2D) square lattice, is that the CCM can also provide information on the quantum order and quantum criticality inherent in this model. We believe that this example illustrates how the CCM is now well placed to study in a very systematic and unbiased manner the quantum phase transitions of the novel non-Fermi-liquid systems discussed above.

2 The CCM for Quantum Spin Lattices

In the single-reference version of the normal (as opposed to the extended [5,7]) variant of the CCM used here we first require a suitable single model or reference state $|\Phi\rangle$, in terms of which a systematic description of the many-body (i.e., in the present case, multi-spin) correlations or fluctuations may be given. We defer till later the important question of how to choose $|\Phi\rangle$ in practice, but simply recall now that it is required only to be a cyclic vector with respect to two well-defined Abelian subalgebras of multi-configurational creation operators $\{C_I^+\}$ and their Hermitian-adjoint destruction counterparts $\{C_I^- \equiv (C_I^+)^\dagger\}$. Thus, $|\Phi\rangle$ plays the role of a vacuum state with respect to a suitable set of (mutually commuting) many-body creation operators $\{C_I^+\}$,

$$C_I^-|\Phi\rangle = 0 \quad , \quad \forall I \neq 0 \quad , \tag{1}$$

with $C_0^- \equiv I$, the identity operator. These operators are also complete in the many-body Hilbert (or Fock) space,

$$I = |\Phi\rangle\langle\Phi| + \sum_{I\neq 0} C_I^+|\Phi\rangle\langle\Phi|C_I^- \quad . \tag{2}$$

The choice of the operators $\{C_I^+\}$ clearly depends on the choice of $|\Phi\rangle$, but for spin-lattice problems in general C_I^+ will involve products of the basic $SU(2)$ spin operators $\{s_k^+, s_k^-, s_k^z\}$ on different lattice sites k, which obey the fundamental commutation relations,

$$[s_k^z, s_l^\pm] = \pm s_k^\pm \delta_{kl} \quad ; \quad [s_k^+, s_l^-] = 2s_k^z\delta_{kl} \quad , \tag{3}$$

where $s_k^\pm \equiv s_k^x \pm is_k^y$. The set-index I will thus generally incorporate the indices for a set of lattice sites. We discuss particular choices of $\{|\Phi\rangle, C_I^+\}$ in more detail below in the context of a specific example.

The exact ground-state energy eigenket and eigenbra vectors, $|\Psi\rangle$ and $\langle\tilde{\Psi}|$ respectively, of a many-body system described by a Hamiltonian H,

$$H|\Psi\rangle = E_g|\Psi\rangle \;\; ; \;\; \langle\tilde{\Psi}|H = E_g\langle\tilde{\Psi}| \;\; , \tag{4}$$

are now specified within the single-reference normal CCM as follows,

$$|\Psi\rangle = e^S|\Phi\rangle \;\; ; \;\; S = \sum_{I\neq 0} \mathcal{S}_I C_I^+ \;\; ,$$

$$\tag{5}$$

$$\langle\tilde{\Psi}| = \langle\Phi|\tilde{\mathcal{S}}e^{-S} \;\; ; \;\; \tilde{S} = 1 + \sum_{I\neq 0} \tilde{\mathcal{S}}_I C_I^- \;\; .$$

The correlation operator S is thus decomposed entirely in terms of the multiconfigurational creation operators $\{C_I^+\}$, and similarly for $\tilde{S}$ in terms of the destruction operators $\{C_I^-\}$. Although the manifest Hermiticity, $(\langle\tilde{\Psi}|)^\dagger = |\Psi\rangle/\langle\Psi|\Psi\rangle$, is lost, the intermediate normalization condition, $\langle\tilde{\Psi}|\Psi\rangle = \langle\Phi|\Psi\rangle = \langle\Phi|\Phi\rangle \equiv 1$ is imposed. Furthermore, the correlation coefficients $\{\mathcal{S}_I, \tilde{\mathcal{S}}_I\}$ are taken as independent variables, even though formally we have the relation,

$$\langle\Phi|\tilde{S} = \frac{\langle\Phi|e^{S^\dagger}e^S}{\langle\Phi|e^{S^\dagger}e^S|\Phi\rangle} \;\; . \tag{6}$$

In particular, the full set of coefficients $\{\mathcal{S}_I, \tilde{\mathcal{S}}_I\}$ provides a complete CCM description of the many-body ground state. For example, an arbitrary operator A has a ground-state expectation value,

$$\bar{A} \equiv \langle\tilde{\Psi}|A|\Psi\rangle = \langle\Phi|\tilde{\mathcal{S}}e^{-S}Ae^S|\Phi\rangle = \bar{A}(\{\mathcal{S}_I, \tilde{\mathcal{S}}_I\}) \;\; . \tag{7}$$

The exponentiated form of the eigenket parametrization of Eq. (5) ensures the proper counting of the ***independent*** fluctuations of excited multi-spin configurations (described by the set-index I) with respect to $|\Phi\rangle$, which are present in the exact ground state $|\Psi\rangle$, and the exact incorporation of the linked cluster theorem of Goldstone. The latter guarantees the size-extensivity of all relevant physical quantities, and allows us to work directly in the thermodynamic limit, $N \to \infty$, where N is the number of lattice spins.

By taking appropriate projections of the ground-state bra and ket Schrödinger equations (i.e., with states $C_I^+|\Phi\rangle$ and $\langle\Phi|C_I^-$, respectively), we obtain coupled sets of equations which may be solved to obtain the coefficients $\{\mathcal{S}_I\}$ and $\{\tilde{\mathcal{S}}_I\}$. Completely equivalently, the correlation coefficients $\{\mathcal{S}_I, \tilde{\mathcal{S}}_I\}$ may be

determined variationally by requiring that the ground-state energy functional $\bar{H}(\{\mathcal{S}_I, \tilde{\mathcal{S}}_I\})$, defined as in Eq. (7), is stationary with respect to variations in each of the (independent) variables of the full set. The following coupled sets of equations are thereby easily derived,

$$\delta\bar{H}/\delta\tilde{\mathcal{S}}_I = 0 \Rightarrow \langle\Phi|C_I^- e^{-S} H e^S|\Phi\rangle = 0 \ , \quad \forall I \neq 0 \ ; \tag{8}$$

$$\delta\bar{H}/\delta\mathcal{S}_I = 0 \Rightarrow \langle\Phi|\tilde{S}e^{-S}[H, C_I^+]e^S|\Phi\rangle = 0 \ , \quad \forall I \neq 0 \ . \tag{9}$$

Equation (8) ensures that the ground-state energy at the stationary point has the simple form

$$E_g = E_g(\{\mathcal{S}_I\}) = \langle\Phi|e^{-S} H e^S|\Phi\rangle \ , \tag{10}$$

which also follows simply by projecting the ground-state ket equation (4) with $\langle\Phi|e^{-S}$. This bi-variational formulation does *not*, however, lead to an upper bound for E_g when the summations over configurations $\{I\}$ in Eq. (5) for S and $\tilde{S}$ are truncated in specific approximations, since the exact Hermiticity between $|\Psi\rangle$ and $\langle\tilde{\Psi}|$ will thereby be lost. On the other hand, the Hellmann-Feynman theorem *is* preserved in all such approximations.

Equation (8) clearly represents a coupled set of nonlinear multinomial equations for the c-number correlation coefficients $\{\mathcal{S}_I\}$. The well-known nested commutator expansion for the similarity-transformed Hamiltonian,

$$\hat{H} \equiv e^{-S} H e^S = H + [H, S] + \frac{1}{2!}[[H, S], S] + \cdots \ , \tag{11}$$

taken together with the fact that all of the individual components of S in the sum in Eq. (5) commute with one another, imply that each element of S in Eq. (5) is thus directly linked to the Hamiltonian in each of the non-vanishing terms in Eq. (11). Each of the coupled set of equations (8) is hence of linked cluster type. What is more, each of these equations is also of finite length when expanded using Eq. (11), since this otherwise infinite series will actually terminate at a finite order here, provided only that each term in the Hamiltonian H contains a finite number of single-site spin operators, as is usually the case. The CCM parametrization thus leads in a very natural way to a workable scheme, which can also be efficiently implemented as described in more detail below.

We turn now to the choice of $|\Phi\rangle$ and the operators $\{C_I^+\}$ for spin-lattice problems. To be specific we restrict ourselves henceforth to spin-$\frac{1}{2}$ quantum antiferromagnets in regions where the corresponding classical limit is described by a generalized Néel-like ordering in which all spins on each sublattice are separately aligned in the coordinates of a global spin quantization axis and

corresponding global spin axes. In such cases it is a simple matter (and see Sec. 3 for specific details in the case considered here) to introduce a different local quantization axis and spin coordinates on each sublattice, by a suitable rotation in spin space, so that the corresponding Néel-like state becomes a fully aligned ("ferromagnetic") state in the local axes. This "ferromagnetic" state is chosen as the uncorrelated CCM model state, $|\Phi\rangle$, in which all spins point, say, along the respective negative z-axis of the corresponding local frames,

$$|\Phi\rangle = \bigotimes_{i=1}^{N} |\downarrow\rangle_i \;\; ; \quad \text{in the local quantization axes.} \tag{12}$$

Thus, in the local spin coordinates,

$$s_k^z|\Phi\rangle = -\frac{1}{2}|\Phi\rangle \;\; , \tag{13}$$

for any arbitrary site k.

The correlation operator S of Eq. (5) may now be decomposed wholly in terms of sums of products of single spin-raising operators, s_k^+, again defined with respect to the local quantization axes. Thus, we may write,

$$\begin{aligned} S &= \sum_{i_1} \mathcal{S}_{i_1} s_{i_1}^+ + \sum_{i_1,i_2} \mathcal{S}_{i_1 i_2} s_{i_1}^+ s_{i_2}^+ + \cdots \\ &= \sum_{n=1}^{N} \sum_{i_1 \cdots i_n} \mathcal{S}_{i_1 \cdots i_n} s_{i_1}^+ \cdots s_{i_n}^+ \;\; , \end{aligned} \tag{14a}$$

where $\mathcal{S}_{i_1 i_2 \cdots i_n}$ are the corresponding (symmetric) spin-correlation coefficients specified by the sets of site indices $\{i_1, i_2, \cdots, i_n\}$ on the regular lattice under consideration. The corresponding expansion for the operator $\tilde{S}$ of Eq. (5) is given by

$$\tilde{S} = 1 + \sum_{n=1}^{N} \sum_{i_1 \cdots i_n} \tilde{\mathcal{S}}_{i_1 \cdots i_n} s_{i_1}^- \cdots s_{i_n}^- \;\; . \tag{14b}$$

The coefficients $\{\mathcal{S}_{i_1 \cdots i_n},\ \tilde{\mathcal{S}}_{i_1 \cdots i_n};\ n = 1, 2, \cdots, N\}$ are hence what we denoted generically by the set $\{\mathcal{S}_I, \tilde{\mathcal{S}}_I\}$ previously. Equation (8) thus yields the specific set of coupled nonlinear CCM equations,

$$\langle \Phi | s_{i_1}^- s_{i_2}^- \cdots s_{i_n}^- e^{-S} H e^{S} | \Phi \rangle = 0 \;\; , \tag{15}$$

to determine the correlation coefficients $\{\mathcal{S}_{i_1 i_2 \cdots i_n}\}$.

We may map the sets of coefficients $\{\mathcal{S}_{i_1 \cdots i_n}\}$ and $\{\tilde{\mathcal{S}}_{i_1 \cdots i_n}\}$ onto sets $\{\mathcal{X}_r\}$ and $\{\tilde{\mathcal{X}}_r\}$ respectively, where r labels the *independent* or fundamental configurations, i.e., only those that are inequivalent under the lattice symmetries (namely, translations, rotations, and reflections) of the Hamiltonian and under permutations of the indices. The sets $\{\mathcal{X}_r\}$ and $\{\tilde{\mathcal{X}}_r\}$ are thus defined to count the independent correlation coefficients associated with each fundamental configuration once and once only. Generally speaking there will be $N\nu_r(n_r)!$ equivalent configurations on the lattice associated with each fundamental configuration, where n_r is the number of sites in the rth configuration and $(n_r)!$ is the combinatoric factor associated with permutations of the n_r indices, the factor N arises from translations, and the factor ν_r is the replication factor of the rth configuration associated with the point symmetry group (or sub-group) of transformations on the lattice which preserve the Hamiltonian. In particular, we need only to consider one of the $N\nu_r(n_r)!$ equivalent sets of equations (15) associated with each independent coefficient $\mathcal{X}_r$.

We now need to consider approximation schemes whereby the expansions of S and $\tilde{S}$ in Eq. (14*a*,*b*) may be truncated to some finite or infinite subset of the full set of independent (fundamental) multi-spin configurations. The three most commonly employed schemes have been: (1) the SUBn scheme, in which all correlations involving only n or fewer spins are retained, but no further restriction is made concerning their spatial separation on the lattice; (2) the SUBn-m sub-approximation, in which all SUBn correlations spanning a range of no more than m adjacent lattice sites are retained; and (3) the localized LSUBm scheme, which retains all multi-spin correlations over all possible distinct locales on the lattice defined by m or fewer contiguous sites. For the results reported below we adopt only the LSUBm scheme here.

The practical implementation of the CCM thus now consists of first enumerating all distinct multi-spin correlation configurations retained in the selected approximation, and then generating the corresponding set of CCM equations. The first stage is essentially a problem in graph theory, whereas Eq. (15) shows that the second stage involves two distinct computational aspects in the calculation of all possible nonzero contributions to the matrix element on the left-hand side of this equation. Thus, the first step is to calculate the similarity-transformed Hamiltonian, $\hat{H} = e^{-S}He^{S}$, and hence $\hat{H}|\Phi\rangle$; while the second is to select those terms of $\hat{H}|\Phi\rangle$ which match exactly the string of spin-lowering operators represented by the set of site indices $\{i_1, i_2, \cdots, i_n\}$, and which hence give a nonzero overlap. Clearly, the former problem is intrinsically related to the noncommutative nature of quantum spin operators, and relies only on the algebraic relations of Eq. (3); while the latter problem is intrinsically related to the geometric properties of the spatial lattice under consideration, and is

essentially a problem of pattern-matching. We have shown elsewhere [29] how each of the above stages may very efficiently be implemented computationally to very high orders, to yield a set of coupled CCM ket-state equations which may then be solved by standard Newton-Raphson techniques. The bra-state equations are also handled in an analogous fashion.

The power of the CCM is illustrated below by application to the spin-$\frac{1}{2}$ anisotropic Heisenberg (or XXZ) model on an infinite 2D square lattice.

3 The Spin-$\frac{1}{2}$ XXZ Antiferromagnet on the 2D Square Lattice

3.1 The Hamiltonian

The XXZ Hamiltonian is specified in terms of global spin coordinates as follows,

$$H = \sum_{\langle i,j \rangle} [s_i^x s_j^x + s_i^y s_j^y + \Delta s_i^z s_j^z] \ , \tag{16}$$

where the sum on $\langle i,j \rangle$ counts all nearest-neighbour pairs once. On the 2D square lattice this model has no exact solution, unlike its 1D chain counterpart which is exactly integrable using the Bethe ansatz. The XXZ model appears to have at least three distinct regimes: an Ising-like phase for sufficiently large values of the anisotropy parameter Δ, which is characterized by nonzero Néel order wherein nearest-neighbour spins in the ground-state wave function align antiparallel along the z-axis; a planar-like phase in which the spins in the ground-state wave function are believed to lie in the xy plane; and a ferromagnetic phase.

Barnes and his co-workers [30] have performed a Monte Carlo study of the 2D XXZ model on a square lattice. They observed that while the staggered magnetization is nonzero in the z-direction for $\Delta > 1$, it appears to fall to zero below $\Delta = 1$. They conclude that there is a phase transition at or very near to the Heisenberg point $\Delta = 1$, exactly as in the 1D case. Kubo and Kishi [31] have also investigated the ground state of the 2D square lattice XXZ model by making use of exact sum rules. They found that the ground state possesses an off-diagonal long-range order similar to that of the XY model at small values of the anisotropy parameter, $0.0 < \Delta < 0.13$. They also found that for values $\Delta > 1.78$ the system possesses nonzero Ising-like long-range order. Finally, at $\Delta = -1$ there is a first-order phase transition to a ferromagnetic phase which exists for all $\Delta < -1$ for this model. Although there are no exact proofs available, it is widely believed that the model has a phase (or perhaps more than one phase) with planar-like order for $-1 < \Delta < 1$, and an Ising-like phase with Néel-like antiferromagnetic order along the z-axis for $\Delta > 1$.

The isotropic Heisenberg point ($\Delta = 1$) is thus expected to be a critical point marking the transition between states of different quantum order. We shall use it here as a specific example to test the ability of the CCM to predict phase transitions and its potential to discuss the critical phenomena (e.g., the critical indices) at this point. For the sake of later comparisons we note that Runge [32] has performed the most accurate Monte Carlo simulations available up till now for the square-lattice spin-$\frac{1}{2}$ isotropic Heisenberg antiferromagnet. By performing simulations on lattices up to size 16×16, and by extrapolating to the infinite lattice limit, $N \to \infty$, he finds a value for the ground-state energy per spin of $E_g/N = -0.66934 \pm 0.00004$, and a value for the sublattice magnetization, M^+, which is $(61.5 \pm 0.5)\%$ of the classical value. By comparison, linear spin-wave theory (LSWT) [33] gives a value of $E_g/N = -0.658$ and a value for M^+ which is 60.6% of the classical value.

3.2 Choice of CCM Model State

There is never a unique choice of model state $|\Phi\rangle$. Our choice should usually be guided by any physical insight available to us concerning the system or, more specifically, that particular phase of it which is under consideration. In the absence of any insight into the quantum many-body system one may sometimes be guided by the behaviour of the corresponding classical system. The XXZ model under consideration provides just such an illustrative example. Thus, for $\Delta > 1$ the *classical* Hamiltonian of Eq. (16) on the 2D square lattice (and, indeed, on any bipartite lattice) is minimized by a perfectly antiferromagnetically Néel-ordered state in the z-direction, whereas for $-1 < \Delta < 1$ it is minimized by a correspondingly ordered state with spins antiferromagnetically aligned along any direction in the xy plane, say along the x-axis. Thus, we see that even for the same spin model and lattice, different choices of model state may be preferable, depending on the particular regime of parameter space in which we are interested. For present purposes we shall utilize both of these classical Néel states, namely the z-aligned Néel state and the x-aligned Néel state (with the latter henceforth denoted as the planar model state), for two separate sets of corresponding CCM calculations. In both cases we now set up different local sets of spin axes on both sublattices so that in the local coordinates all spins in both model states point in the negative z-direction, as discussed above in Sec. 2 [and see Eq. (12)].

For the z-aligned Néel state we simply perform a rotation of the axes of the up-pointing spins by 180^o about the y-axis, such that

$$s^x \to -s^x, \quad s^y \to s^y, \quad s^z \to -s^z \quad . \tag{17}$$

The Hamiltonian of Eq. (16) may then be written in these local axes as

$$H^z = -\frac{1}{2}\sum_{\langle i,j\rangle}\left[s_i^+ s_j^+ + s_i^- s_j^- + 2\Delta s_i^z s_j^z\right] \quad , \tag{18}$$

where the superscript z on H^z reminds us that the Hamiltonian is written in the local spin coordinate axes appropriate to the z-aligned Néel model state.

In order to produce a "ferromagnetic" model state, as in Eq. (12), for the planar model state in the local frames, we rotate the axes of the left-pointing spins (i.e., those pointing in the negative x-direction) in the planar state by 90^o about the y-axis, and the axes of the corresponding right-pointing spins by -90^o about the y-axis. (Note that the positive z-axis is defined here to point upwards and the positive x-axis is defined to point rightwards.) Thus, the transformations of the local axes are described such that

$$s^x \to s^z \quad , \quad s^y \to s^y \quad , \quad s^z \to -s^x \tag{19}$$

for the left-pointing spins, and such that

$$s^x \to -s^z \quad , \quad s^y \to s^y \quad , \quad s^z \to s^x \tag{20}$$

for the right-pointing spins. The transformed Hamiltonian of Eq. (16) may now be written in these local axes as

$$H^p = -\frac{1}{4}\sum_{\langle i,j\rangle}\left[(\Delta+1)(s_i^+ s_j^+ + s_i^- s_j^-) + (\Delta-1)(s_i^+ s_j^- + s_i^- s_j^+) + 4s_i^z s_j^z\right] \quad , \tag{21}$$

where, again, the superscript p on H^p reminds us that the Hamiltonian is written in the local spin coordinate axes appropriate to the planar model state. It is important to recall that since the Hamiltonians H, H^z, and H^p of Eqs. (16), (18), and (21) differ only by similarity transformations their eigenvalue spectra are identical.

3.3 Enumeration of the Independent Correlation Configurations

The first step in the practical implementation of the CCM at the LSUBm level of approximation discussed in Sec. 2 is to enumerate all of the distinct multi-spin configurations or correlated clusters, which we shall henceforth call *fundamental* configurations, $\{i_1, i_2, \cdots, i_n\}$ with $n < m$, which are retained at the LSUBm level. Only those configurations which cannot be obtained from one another using the lattice symmetries (namely, translations, rotations and reflections) shared by the Hamiltonian are to be counted as distinct. For

the square lattice under consideration there are four rotational operations, $(0°, 90°, 180°, 270°)$, and four reflections, (along the x and y axes, and along the lines $y = \pm x$), which preserve the symmetries of both the lattice and the Hamiltonian. Each such fundamental configuration is associated with two single independent correlation coefficients $\mathcal{X}_r$ and $\tilde{\mathcal{X}}_r$ associated with the cluster operators S and $\tilde{S}$ respectively, as discussed in Sec. 2. Each correlated cluster may be either a connected cluster of size m (also known as a "lattice animal" or "polyomino") or a connected or disconnected subset of it. We note that the enumeration of the number of lattice animals of size m on a regular lattice as m becomes large remains an open problem in combinatorial graph theory. However, efficient algorithms for their enumeration for $m \lesssim 20$ have been developed in such fields as cell growth and percolation theory.

Although H^p and H^z are fully equivalent to one another, the number of fundamental LSUBm configurations at each level $m > 2$ is greater for H^p than for H^z due to other constraints which arise from symmetries of the Hamiltonian. Thus, firstly, we note that both H^p and H^z contain only even products of spin-flip operators (plus a single term containing two s^z operators). Repeated application of either Hamiltonian to the model state $|\Phi\rangle$ will thus only create states with an even number of spin flips with respect to it. Since the exact ground state may be obtained as a linear combination of states obtained by repeated application of the Hamiltonian to $|\Phi\rangle$, assuming only that $|\Phi\rangle$ is not orthogonal to the exact ground state, we may hence restrict ourselves to LSUBm fundamental configurations which contain an even number of spin flips, i.e., to coefficients $\mathcal{S}_{i_1 i_2 \cdots i_n}$ where n is even.

Secondly, we note that the number of fundamental configurations can be further reduced for H^z. Thus, H^z has the additional feature that when applied to $|\Phi\rangle$ it produces states with the same number of spin flips on both sublattices, and hence we can further restrict the fundamental configurations to those which preserve this feature. This symmetry is related to the fact that the original Hamiltonian, and hence also H^p and H^z, commute with the z-component of the total uniform magnetization, $s^z_T = \sum_i s^z_i$ (where s^z_i is defined with respect to the original global quantization axis, and the sum over the index i runs over all $N \to \infty$ lattice sites). However, whereas the z-aligned Néel model state is an eigenstate of s^z_T, the planar model state is not. Hence, for the z-aligned Néel model state one may explicitly conserve s^z_T (as zero for the antiferromagnetic sector) by restricting the fundamental configurations to those which produce no change in s^z_T $(= 0)$. We note the number of fundamental configurations up to the LSUB8 level of approximation for both model states in Table 1. The actual calculations reported below are performed up to this level for H^z, but only up to LSUB6 level for H^p due to the increased number of fundamental

configurations in the latter case.

We note also that H^p and H^z become identical at the Heisenberg point $\Delta = 1$. In the actual calculations this is reflected by the fact that the additional cluster correlation coefficients at a given LSUBm level included for H^p beyond those included for H^z become zero at this point, $\Delta \rightarrow 1^-$. Further details of the enumeration of the independent configurations is contained in Ref. [29].

3.4 The CCM Ket-State Equations

In order to evaluate the CCM ket-state equations (15), we first require the similarity-transformed Hamiltonians, $\hat{H}^z$ and $\hat{H}^p$, defined as in Eq. (11). By making use of the fundamental $SU(2)$ commutation relations of Eq. (3) it is straightforward to show that after letting $\hat{H}^z$ act on $|\Phi\rangle$, as needed in Eq. (15), we have

$$\hat{H}^z|\Phi\rangle \equiv e^{-S}H^z e^S|\Phi\rangle = \left(\hat{H}_1^z + \hat{H}_2^z + \hat{H}_3^z\right)|\Phi\rangle \quad , \tag{22}$$

where

$$\hat{H}_1^z = -\frac{1}{2}\Delta \sum_{k\rho} \left(F_k^z F_m^z + G_{km}^z\right) s_k^+ s_m^+$$

$$-\frac{1}{4}\sum_{k\rho}\left[1 + \left(F_k^z\right)^2\left(F_m^z\right)^2 + 4F_k^z F_m^z G_{km}^z + 2\left(G_{km}^z\right)^2\right] s_k^+ s_m^+ \quad , \tag{23}$$

$$\hat{H}_2^z = \frac{1}{4}\Delta \sum_{k\rho}\left(F_k^z s_k^+ + F_m^z s_m^+\right) + \frac{1}{4}\sum_{k\rho}\left(F_k^z F_m^z + 2G_{km}^z\right)\left(F_k^z s_k^+ + F_m^z s_m^+\right) \quad , \tag{24}$$

$$\hat{H}_3^z = -\frac{1}{8}\sum_{k\rho}\left[\Delta + 2\left(F_k^z F_m^z + G_{km}^z\right)\right] \quad , \tag{25}$$

and where k runs over all lattice sites, and $m \equiv k + \rho$ such that ρ runs over all 4 nearest neighbours to k on the lattice. The operators F_k and G_{km} are defined generically as follows,

$$F_k \equiv \sum_{l=1}^{\infty} \sum_{i_1 \cdots i_{l-1}} \mathcal{S}_{k i_1 \cdots i_{l-1}} s_{i_1}^+ \cdots s_{i_{l-1}}^+ \quad , \tag{26}$$

$$G_{km} \equiv \sum_{l=2}^{\infty} l\,(l-1) \sum_{i_1 \cdots i_{l-2}} \mathcal{S}_{k m i_1 \cdots i_{l-2}} s_{i_1}^+ \cdots s_{i_{l-2}}^+ \quad , \tag{27}$$

and F_k^z and G_{km}^z are the particular cases where $\mathcal{S}_{i_1 \cdots i_n} \rightarrow \mathcal{S}_{i_1 \cdots i_n}^z$, namely the cluster correlation coefficients obtained by use of the present z-aligned

Néel state and H^z. Equation (25) shows that the ground-state energy for the z-aligned Néel model state is simply given in terms of $x_1^z \equiv \mathcal{S}^z_{k,k+\rho}$, the nearest-neighbour two-body cluster correlation coefficient obtained by using H^z and the z-aligned Néel model state, as

$$\frac{E_g}{N} = -\frac{1}{2}\left(4x_1^z + \Delta\right) \quad . \tag{28}$$

We note that $x_1^z \equiv \mathcal{S}^z_{k,k+\rho}$ is independent of k and ρ by the translational and rotational symmetries of the lattice.

The equivalent relations for $\hat{H}^p$ are obtained as follows,

$$\hat{H}^p|\Phi\rangle \equiv e^{-S}\hat{H}^p e^S|\Phi\rangle = \left(\hat{H}_1^p + \hat{H}_2^p + \hat{H}_3^p\right)|\Phi\rangle \quad , \tag{29}$$

where

$$\hat{H}_1^p = \frac{1}{2}\sum_{k\rho}\left\{-(F_k^p F_m^p + G_{km}^p) + \frac{1}{4}(\Delta-1)\left[(F_k^p)^2 + (F_m^p)^2\right]\right\} s_k^+ s_m^+$$

$$-\frac{1}{8}(\Delta+1)\sum_{k\rho}\left[1 + (F_k^p)^2\,(F_m^p)^2 + 4F_k^p F_m^p G_{km}^p + 2\,(G_{km}^p)^2\right] s_k^+ s_m^+ \quad , \tag{30}$$

$$\hat{H}_2^p = \frac{1}{4}\sum_{k\rho}\left[F_k^p s_k^+ + F_m^p s_m^+ + \frac{1}{2}(1-\Delta)\left(F_k^p s_m^+ + F_m^p s_k^+\right)\right]$$

$$+\frac{1}{8}(\Delta+1)\sum_{k\rho}(2G_{km}^p + F_k^p F_m^p)\left(F_k^p s_k^+ + F_m^p s_m^+\right) \quad , \tag{31}$$

$$\hat{H}_3^p = -\frac{1}{8}\sum_{k\rho}[1 + (\Delta+1)(F_k^p F_m^p + G_{km}^p)] \quad . \tag{32}$$

The operators F_k^p and G_{km}^p are again defined as in Eqs. (26) and (27), but with the cluster correlation coefficients $\mathcal{S}_{i_1\cdots i_n} \rightarrow \mathcal{S}^p_{i_1\cdots i_n}$ obtained by use of the present planar model state and H^p. Equation (32) immediately yields,

$$\frac{E_g}{N} = -\frac{1}{2}\left[2x_1^p(\Delta+1) + 1\right] \quad , \tag{33}$$

where $x_1^p \equiv \mathcal{S}^p_{k,k+\rho}$, the nearest-neighbour two-body cluster correlation coefficient obtained by using H^p and the planar model state.

In both cases the corresponding LSUBm equations are obtained by evaluating all nonzero contributions to Eq. (15). There is one such (coupled nonlinear)

equation for every fundamental configuration retained, and hence N_F equations in N_F coefficients, for each level of approximation. The actual derivation of the ket-state equations from Eq. (15) and Eqs. (22)-(25) or Eqs. (29)-(32) is thus seen to reduce essentially to a pattern-matching exercise, and we describe elsewhere [29] its efficient computational implementation. The bra-state equations can also be derived in an analogous fashion.

4 Results

4.1 Ground-State Energy

Results for the ground-state energy using the two model states are illustrated in Fig. 1 at the LSUB4 and LSUB6 levels of approximation, where they are compared with the Monte Carlo results of Barnes *et al.* [30]. The highest approximation that we have undertaken for the planar model state case is LSUB6, which contains 131 independent cluster configuration coefficients and which yields an energy per spin, $E_g/N = -0.66700$ at the Heisenberg point ($\Delta = 1$). Due to the reduced number of independent configurations for the case of the z-aligned Néel model state we have also been able to solve the higher LSUB8 approximation in this case. The 1287 coupled equations in this case yield a value of the energy per spin, $E_g/N = -0.66817$ at $\Delta = 1$. The results for the Heisenberg model (which are identical using both model states for this case) are summarized in Table 1, and ground-state energies are also shown in Table 2 for a range of values of Δ, and for calculations using both model states as CCM reference states.

In order to compare our results with those cited in Sec. 3.1 from other methods, we attempt a simple heuristic extrapolation of our LSUBm results to the limit $m \to \infty$ at the isotropic Heisenberg point ($\Delta = 1$). As has already been found elsewhere [11], our results seem to extrapolate well to their asymptotic value with a leading m-dependent correction that scales as m^{-2}. In this way we obtain an extrapolated value for the ground-state energy per spin of $E_g/N = -0.66968$. This compares very well with the best Monte Carlo simulation value [32] of -0.66934 ± 0.00004, and is very much more accurate, by comparison with this Monte Carlo value, than the linear spin-wave theory (LSWT) result [33] of $E_g/N = -0.658$.

Figure 1 and Table 2 illustrate that at a given LSUBm level of approximation the CCM result for the ground-state energy using the z-aligned Néel model state lies lower than its counterpart using the planar model state for $\Delta > 1$, and *vice versa* for $\Delta < 1$. This result is precisely as would be expected classically, as discussed above in Sec. 3.2, and it illustrates the power of being

Table 1: Results obtained for the spin-$\frac{1}{2}$ XXZ model on the 2D square lattice using CCM LSUBm approximations ($m = 2, 4, 6, 8$). N_F^p denotes the number of fundamental configurations for the planar model state, and N_F^z denotes the number of fundamental configurations for the z-axis Néel model state. The ground-state energy per spin, E_g/N, and the sublattice magnetisation, M^+, at the isotropic Heisenberg point ($\Delta = 1$) are shown, as well as extrapolated results in the limit $m \to \infty$. Various critical anisotropy parameters are also given. Δ_F^p and Δ_A^p indicate the LSUBm critical points for the planar model state corresponding to the ferromagnetic and antiferromagnetic phase transitions. Δ_A^z indicates the critical point for the z-axis Néel model state corresponding to the antiferromagnetic phase transition. Note that there are no terminating points in the LSUB2 approximation.

m	N_F^p	N_F^z	$\frac{E_g}{N}\vert_{\Delta=1}$	$M^+\vert_{\Delta=1}$	Δ_F^p	Δ_A^p	Δ_A^z
2	1	1	−0.64833	0.8414	–	–	–
4	10	7	−0.66366	0.7648	−1.250	1.648	0.577
6	131	75	−0.66700	0.7273	−1.084	1.286	0.7631
8	2793	1287	−0.66817	0.7048	?	?	0.8429
∞	–	–	−0.66968	0.62	−0.95	1.00	0.96±0.04

able to employ different CCM model states which are specifically geared to different possible phases. If we were simply to take that solution with the lower energy for each value of Δ (for which we note, however, that there is no real justification), we would infer that there is a phase transition at $\Delta = 1$ between a phase with Ising-like order at $\Delta > 1$ and a planar-like phase for $\Delta < 1$.

We note, furthermore, and much more importantly, that each separate calculation also yields evidence of such a phase transition. Thus, we find that beyond certain critical values, Δ_c, of the anisotropy parameter there exists no physically reasonable solution to the LSUBm CCM equations for $m \geq 4$, as is illustrated for the cases $m = 4, 6$ in Fig. 1. In previous work [11] we have related this characteristic breakdown of the CCM equations at certain critical points to actual phase transitions of the real system, and we explore this further in Sec. 4.2 below. A useful means to detect phase transitions within the LSUBm scheme is to calculate the so-called anisotropy susceptibility, χ_a,

$$\chi_a \equiv -\frac{\partial^2(E_g/N)}{\partial\Delta^2} \quad , \tag{34}$$

Since the CCM equations are known analytically, χ_a and all other derivatives may also be calculated *directly* (i.e., from analytic equations). We find that χ_a diverges at the critical points.

More specifically, we find that for the CCM calculations based on the planar model state χ_a diverges at critical values $\Delta_c = \Delta_F^p$ and Δ_A^p, corresponding

Table 2: Results for the ground-state energy per spin of the 2D spin-$\frac{1}{2}$ XXZ model on the square lattice using both the planar and z-aligned Néel model states, compared with the Monte Carlo results of Ref. [30]. The '–' symbol indicates values of Δ which lie outside the range, defined by the Δ_F^p, Δ_A^p, and Δ_A^z critical points, in which there exists a physically reasonable solution to the LSUBm CCM equations for $m \geq 4$. The '**' symbol indicates points at which a Monte Carlo solution has not yet been determined.

Δ	CCM results based on the planar Néel state		Monte Carlo	CCM results based on the z-aligned Néel state		
	LSUB4	LSUB6		LSUB8	LSUB6	LSUB4
-1.0	−0.5	−0.5	**	–	–	–
-0.5	−0.5145	−0.5151	**	–	–	–
0.0	−0.5473	−0.5483	**	–	–	–
0.5	−0.5959	−0.5975	**	–	–	–
0.71429	−0.6222	−0.6242	−0.624	–	–	−0.5891
0.83333	−0.6385	−0.6408	−0.641	–	−0.6199	−0.6116
0.90909	−0.6496	−0.6523	−0.652	−0.6415	−0.6390	−0.6338
0.95238	−0.6562	−0.6591	−0.661	−0.6535	−0.6518	−0.6477
1.0	−0.6637	−0.6670	−0.669	−0.6682	−0.6670	−0.6637
1.05263	−0.6723	−0.6762	−0.687	−0.6856	−0.6848	−0.6821
1.11111	−0.6823	−0.6871	−0.704	−0.7062	−0.7056	−0.7035
1.17647	−0.6940	−0.7005	−0.729	−0.7303	−0.7298	−0.7282
1.25	−0.7082	−0.7189	−0.759	−0.7585	−0.7582	−0.7570
1.5	−0.7680	–	**	−0.8611	−0.8610	−0.8604
2.0	–	–	**	−1.0833	−1.0833	−1.0831

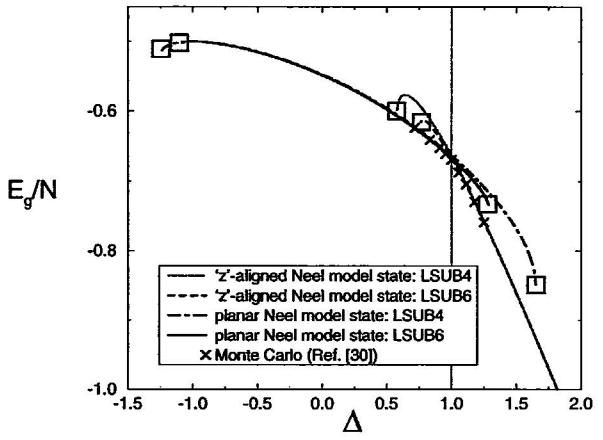

Figure 1: Results for the CCM ground-state energy of the spin-$\frac{1}{2}$ XXZ model on the 2D square lattice, using the LSUBm approximation with $m = 4, 6$ based on both the planar and z-aligned Néel model states, compared to the Monte Carlo results of Ref. [30]. LSUBm critical points, Δ_F^p, Δ_A^p and Δ_A^z, are indicated by the boxes.

to the ferromagnetic and antiferromagnetic phase transitions respectively, for all LSUBm approximations with $m > 2$. These results are illustrated in Table 1, which also displays the single critical point at $\Delta_c = \Delta_A^z$ for the CCM calculations based on the z-aligned Néel model state, and which again corresponds to the antiferromagnetic phase transition. As one might hope, the position of the critical point Δ_F^p becomes closer to the true ferromagnetic phase transition at $\Delta = -1$ as the approximation level is increased. Also, both Δ_A^p and Δ_A^z appear to converge with increasing LSUBm index m, and for a given value of m always bound the point $\Delta = 1$ at which the true antiferromagnetic phase transition is believed (by symmetry arguments) to lie. We have shown elsewhere [11] how the corresponding SUB2-m results for Δ_A^z seem to approach the full SUB2 value as m^{-2}, and the same rule fitted to the LSUBm results yields the corresponding predictions for the extrapolated antiferromagnetic point indicated in Table 1, namely $\Delta_A^z \approx 0.96 \pm 0.04$, and $\Delta_A^p \approx 1.00$. Both predictions are compatible with each other and with the expected value $\Delta_A = 1$.

4.2 Sublattice Magnetization

In order to discuss the phase transition further it is necessary to consider the degree of quantum order inherent in the CCM wave functions obtained at the various LSUBm levels of approximation, and based on both model states. The simplest such order parameter is the sublattice magnetization, $M^+ \equiv -2\langle s^z \rangle$, which is defined as the average over the entire lattice of s^z in the *local* (rotated) spin coordinates, or, equivalently over a single sublattice of the corresponding unrotated component of the spin in the original *global* coordinates. Thus, $M^+ = 1$ for both model states, with perfect antiferromagnetic alignment along the global z-axis for the z-aligned state and along the global x-axis for the planar state. Quantum fluctuations (i.e., multi-spin correlations) present in the exact interacting ground state are expected to reduce M^+ below unity. We would expect, *a priori*, that a phase transition would be marked by M^+ becoming zero (or, in an approximate calculation, singular) at some critical value of the coupling parameter, namely Δ for the present XXZ model.

By inserting the CCM parametrizations of Eq. (5) we find,

$$M^+ = -\frac{2}{N}\sum_{k=1}^{N}\langle\tilde{\Psi}|s_k^z|\Psi\rangle = -\frac{2}{N}\sum_{k=1}^{N}\langle\Phi|\tilde{S}e^{-S}s_k^z e^{S}|\Phi\rangle \quad , \tag{35}$$

where s_k^z is in the local coordinates of each sublattice. In the notation of Eq. (26) we find

$$\begin{aligned} M^+ &= 1 - \frac{2}{N}\sum_{k=1}^{N}\langle\Phi|\tilde{S}F_k s_k^+|\Phi\rangle \\ &= 1 - \frac{2}{N}\sum_{n=1}^{\infty} n(n!)\sum_{i_1\cdots i_n}\tilde{\mathcal{S}}_{i_1\cdots i_n}\mathcal{S}_{i_1\cdots i_n} \quad . \end{aligned} \tag{36}$$

The sum in Eq. (36) may be rewritten in terms of the independent correlation coefficients $\tilde{\mathcal{X}}_r$ and $\mathcal{X}_r$ associated with the N_F fundamental configurations of a given LSUBm approximation, which were introduced in Sec. 2, to give the LSUBm estimate for M^+,

$$\begin{aligned} M^+ &= 1 - 2\sum_{r=1}^{N_F} n_r(n_r!)^2\nu_r\tilde{\mathcal{X}}_r\mathcal{X}_r \\ &= 1 - 2\sum_{r=1}^{N_F} n_r(n_r!)\tilde{x}_r x_r \quad , \end{aligned} \tag{37}$$

where n_r is the number of spin flips with respect to $|\Phi\rangle$ for the rth fundamental configuration, and where we have introduced the notation $x_r \equiv \mathcal{X}_r$ and $\tilde{x}_r \equiv (n_r!)\nu_r\tilde{\mathcal{X}}_r$. For the square lattice considered here $\nu_r = 4$ or 8 for all allowed fundamental configurations.

Evaluation of the sublattice magnetization requires both the ket- and bra-state cluster correlation coefficients. We have described the computation of the ket-state coefficients in broad outline above. The bra-state coefficients are calculated similarly, by making use of the generic linear equations (9), once the ket-state coefficients are known. The actual procedure is straightforward, and is also described in more detail elsewhere [29].

Results for M^+ for the spin-$\frac{1}{2}$ 2D XXZ model on the square lattice using both CCM model states are shown in Fig. 2. Table 1 summarizes the results at the isotropic Heisenberg point, $\Delta = 1$. We note again that the corresponding LSUBm results for M^+ at a given truncation level m are identical at $\Delta = 1$. We see that over the entire range $-1 < \Delta < 1$ our results seem to converge well to a nonzero in-plane long-range order, with a nonzero planar sublattice magnetization, whereas for all $\Delta > 1$ we have comparable nonzero long-range order along the spin z-axis and a nonzero z-component of sublattice magnetization. The divergence in M^+ near the critical points Δ_A^z and Δ_A^p strongly reinforces our interpretation of these points as reflecting a phase transition. As we approach one of these antiferromagnetic critical points for a given LSUBm approximation, we typically find that at least one of the CCM correlation coefficients x_r becomes very large, and hence M^+ diverges from Eq. (36).

We again attempt a simple heuristic extrapolation of our LSUBm results for M^+ at the Heisenberg point ($\Delta = 1$) to the limit $m \to \infty$, in order to compare our results with those from other calculations. As has been found elsewhere [11] the results for M^+ extrapolate well to their asymptotic value with a leading correction that scales as m^{-1}. As shown in Table 1 we thus obtain an extrapolated value, $M^+ = 0.62$. This compares extremely well with the best available Monte Carlo simulation value of Runge [32], $M^+ = 0.615 \pm 0.005$, and with the value $M^+ = 0.62 \pm 0.02$ from series expansion techniques [34].

4.3 Critical Properties

We have demonstrated so far that CCM calculations using the LSUBm approximation scheme based on different model states are well able to describe both the Ising-like phase for $\Delta > 1$ and the planar-like phase for $-1 < \Delta < 1$ of the spin-$\frac{1}{2}$ 2D XXZ model on the square lattice. The results are not only extremely accurate for such quantities as the ground-state energy and sublattice

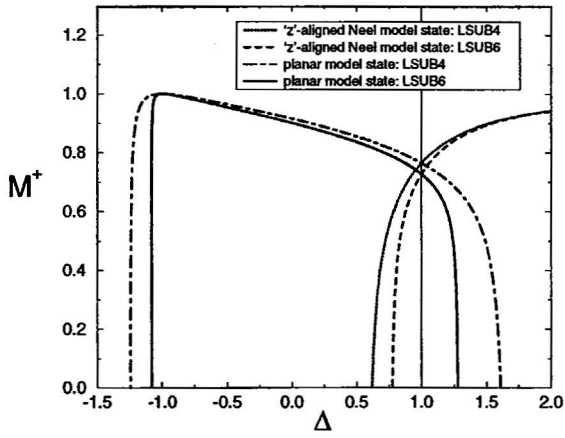

Figure 2: Results for the CCM sublattice magnetization M^+ of the spin-$\frac{1}{2}$ XXZ model on the 2D square lattice using the LSUBm approximation with $m = 4, 6$ based on both the planar and z-aligned Néel model states. The results indicate nonzero long-range order in the xy plane for $-1 < \Delta < 1$, and along the z-axis for $\Delta > 1$.

magnetization as functions of Δ, but calculations based on each model state separately give accurate results for the critical values Δ_c which delimit the regime in Δ in which that model state is apposite. These critical values clearly mark (at the level of approximation considered) the physical phase boundaries. We show below, by specific application to the same spin-$\frac{1}{2}$ square-lattice XXZ model, that our CCM formalism also has the power to predict the critical behaviour of the physical observables near such phase transitions, i.e., that we can extract from the LSUBm results useful information on critical indices.

Thus, the critical index for the singular (non-analytic) term in E_g/N near an LSUBm critical point $\Delta_c(m)$ can first be obtained, for example, by direct examination of the anisotropy susceptibility, $\chi_a \equiv -\partial^2(E_g/N)/\partial\Delta^2$, of Eq. (34). For $m > 2$ we find,

$$\chi_a^m(\Delta) \longrightarrow \bar{\chi}_a^m |\Delta - \Delta_c(m)|^{-\alpha_0} \quad ; \quad \Delta \rightarrow \Delta_c(m) \quad . \tag{38}$$

Direct calculation for the LSUBm approximations using both the z-aligned and planar Néel model states shows that for $m > 2$ we have $\alpha_0 \approx 1.500 \pm 0.005$. However, the prefactors $\bar{\chi}_a^m$ in Eq. (38) are themselves strongly dependent on the truncation index m. We may now use a variant of the so-called coherent

anomaly method (CAM) of Suzuki [35] to extract further information. Thus, we attempt to fit $\bar{\chi}_a^m$ with the coherent anomaly form,

$$\bar{\chi}_a^m \longrightarrow K|\Delta_c(\infty) - \Delta_c(m)|^{\nu} \;\; ; \quad \Delta \rightarrow \Delta_c(\infty) \;\; , \tag{39}$$

where K is a constant. Thus, as explained by Suzuki [35], one may intuit or prove that the exact $\chi_a(\Delta)$ has the critical form,

$$\chi_a(\Delta) \longrightarrow \kappa|\Delta - \Delta_c(\infty)|^{-\alpha_0+\nu} \;\; ; \quad \Delta \rightarrow \Delta_c(\infty) \equiv \Delta_c \;\; , \tag{40}$$

where κ is a constant.

A CAM analysis along these lines of the LSUBm results based on the z-aligned Néel state gives $\nu \approx 1.25$ using the $\Delta_A^z(4)$ and $\Delta_A^z(6)$ data, and $\nu \approx 0.97$ using the $\Delta_A^z(6)$ and $\Delta_A^z(8)$ data. We thus obtain a singular term in E_g/N near Δ_A^z with a critical exponent $2 - \alpha_0 + \nu \approx 1.50 - 1.75$. This may be compared with the corresponding value of $3/2$ for both the mean-field-like CCM SUB2 approximation (in which *all* 2-spin-flip correlation terms are retained, however far apart on the lattice) and linear spin-wave theory (LSWT). A corresponding analysis may also be carried out on the LSUBm results based on the planar model state near Δ_A^p. We again find $\alpha_0 \approx 1.500 \pm 0.005$ for both the LSUB4 and LSUB6 results, and a corresponding critical anomaly based on these of $\nu \approx 1.27$. We thus obtain a singular term in E_g/N near Δ_A^p with a critical exponent $2 - \alpha_0 + \nu \approx 1.77$. These preliminary data are clearly compatible with the hypothesis that the critical exponent in the energy is the same on both sides of the antiferromagnetic phase transition Δ_A.

Similar CAM analyses can also be performed for the ground-state energy near the corresponding ferromagnetic critical point Δ_F^p, and for such other properties as the sublattice magnetization M^+ near any of these critical points.

5 Conclusions

Our aim has been to show that the coupled cluster method of microscopic quantum many-body theory may be used to great advantage to study quantum spin-lattice models at a level which includes the quantitative identification of zero-temperature quantum phase transition points between states of different magnetic ordering, and the various critical indices which describe their behaviour in the vicinity of these transitions. The CCM is now in the position of being virtually the only fully microscopic method available which can yield very accurate results for both local ground-state properties and the global critical behaviour of these highly correlated systems.

For spin-lattice models with nearest-neighbour interactions on bipartite lattices, such as the XXZ model considered here, quantum Monte Carlo results

are also available. The infamous "minus-sign problem" which bedevils Monte Carlo simulations can be circumvented for these models by mapping them onto equivalent bosonic problems or, equivalently, by utilizing the Marshall sign rule [36] concerning the phase relations between the projection coefficients of the ground-state wave function onto a complete set of spin configurations. We have seen that our own CCM formalism can be effectively implemented computationally to levels where the results are comparable in accuracy to the best Monte Carlo results for these cases.

By contrast, for *frustrated* models (e.g., models with both nearest-neighbour and next-nearest-neighbour interactions [12,24,25], or the same XXZ model considered here but on a 2D triangular lattice [13]) Monte Carlo simulations are much more difficult to implement (e.g., see Ref. [37] for the typical case of the isotropic spin-$\frac{1}{2}$ Heisenberg model on a triangular lattice). On the other hand, as we have shown elsewhere [12,13,24,25], the CCM is no more difficult to implement, either in principle or in practice, for such frustrated systems. In particular, there is now a real hope that the CCM results can provide better trial wave functions with more accurate nodal surface structure for more ambitious fixed-node-type Monte Carlo simulations of such systems.

Further extensions of our CCM formalism may be envisaged. For example, LSUBm calculations on spin lattices where the spins have quantum number $s > \frac{1}{2}$ present no real difficulty [10(f)]. Thus, one merely generalizes to the case of "multiple occupancy" of the sites $\{i_1, \cdots, i_n\}$ in the retained fundamental configurations, where each site can now be "occupied" up to $2s$ times. We are hopeful that our general methodology can be applied to other unconventional (non-Fermi-liquid-type) systems of the sort discussed in Sec. 1. Systems which seem particularly ripe for application of the CCM techniques considered here include the valence-bond solids [24,26] and lattice models with electronic degrees of freedom, such as the Hubbard model [17,27].

It would also be of interest to extend the CCM treatment of each of the above models, including the XXZ model considered here, to finite temperatures. One obvious way to do this would be to extend the formalism by utilizing the general framework of thermofield dynamics [38]. Mukherjee [39] and others have suggested alternative ways to extend the CCM to incorporate a thermal averaging procedure.

Acknowledgements

We thank J.B. Parkinson, Y. Xian, and C. Zeng for useful discussions. One of us (RFB) also gratefully acknowledges a research grant from the Engineering and Physical Sciences Research Council (EPSRC) of Great Britain.

References

1. F. Coester, *Nucl Phys.* **7**, 421 (1958); F. Coester and H. Kümmel, *ibid.* **17**, 477 (1960).
2. J. Čižek, *J. Chem. Phys.* **45**, 4256 (1966); *Adv. Chem. Phys.* **14**, 35 (1969).
3. R.F. Bishop and K.H. Lührmann, *Phys. Rev. B* **17**, 3757 (1978).
4. H. Kümmel, K.H. Lührmann, and J.G. Zabolitzky, *Phys. Rep.* **36C**, 1 (1978).
5. J.S. Arponen, *Ann. Phys. (N.Y.)* **151**, 311 (1983).
6. R.F. Bishop and H. Kümmel, *Phys. Today* **40(3)**, 52 (1987).
7. J.S. Arponen, R.F. Bishop, and E. Pajanne, *Phys. Rev. A* **36**, 2519 (1987); *ibid.* **36**, 2539 (1987); in *Condensed Matter Theories,* (eds. P. Vashishta, R.K. Kalia, and R.F. Bishop), Plenum, New York, 1987, Vol. **2**, p. 357.
8. R.J. Bartlett, *J. Phys. Chem.* **93**, 1697 (1989).
9. R.F. Bishop, *Theor. Chim. Acta* **80**, 95 (1991).
10. R.F. Bishop, J.B. Parkinson, and Yang Xian, (a) *Phys. Rev. B* **43**, 13782 (1991); (b) *ibid.* **44**, 9425 (1991); (c) *ibid.* **46**, 880 (1992); (d) *Theor. Chim. Acta* **80**, 181 (1991); (e) *J. Phys.: Condens. Matter* **4**, 5783 (1992); (f) *ibid.* **5**, 9169 (1993).
11. R.F. Bishop, R.G. Hale, and Y. Xian, *Phys. Rev. Lett.* **73**, 3157 (1994).
12. D.J.J. Farnell and J.B. Parkinson, *J. Phys.: Condens. Matter* **6**, 5521 (1994).
13. C. Zeng, I. Staples, and R.F. Bishop, (a) *J. Phys.: Condens. Matter* **7**, 9021 (1995); (b) *Phys. Rev. B* **53**, 9168 (1996).
14. R.F. Bishop, D.J.J. Farnell, and J.B. Parkinson, *J. Phys.: Condens. Matter* **8**, 11153 (1996).
15. R.F. Bishop and Y. Xian, in *Condensed Matter Theories,* (eds. J.W. Clark, K.A. Shoaib, and A. Sadiq), Nova Science Publ., Commack, New York, 1994, Vol. **9**, p. 433.
16. R.F. Bishop, in *Recent Progress in Many-Body Theories,* (eds. E. Schachinger, H. Mitter, and H. Sormann), Plenum, New York, 1995, Vol. **4**, p. 195.
17. R.F. Bishop, Y. Xian, and C. Zeng, *Int. J. Quantum Chem.* **55**, 181 (1995).
18. R.F. Bishop and Y. Xian, *Acta Phys. Polonica B* **24**, 541 (1993); R.F. Bishop, A.S. Kendall, L.Y. Wong, and Yang Xian, *Phys. Rev. D* **48**, 887 (1993); R.F. Bishop and Y. Xian, *Nucl. Phys. B (Proc. Suppl.)* **34**, 808 (1994); N.J. Davidson and R.F. Bishop, *ibid.* **42**, 817 (1995); S.J. Baker,

R.F. Bishop, and N.J. Davidson, *ibid.* **53**, 834 (1997).
19. M. Roger and J.H. Hetherington, *Phys. Rev. B* **41**, 200 (1990).
20. C.F. Lo, K.K. Pang, and Y.L. Wang, *J. Appl. Phys.* **70**, 6080 (1991).
21. F.E. Harris, *Phys. Rev. B* **47**, 7903 (1993).
22. F. Cornu, Th. Jolicoeur, and J.C. Le Guillou, *Phys. Rev. B* **49**, 9548 (1994).
23. W.H. Wong, C.F. Lo, and Y.L. Wang, *Phys. Rev. B* **50**, 6126 (1994).
24. Y. Xian, *J. Phys.: Condens. Matter* **6**, 5965 (1994).
25. R. Bursill, G.A. Gehring, D.J.J. Farnell, J.B. Parkinson, T. Xiang, and C. Zeng, *J. Phys.: Condens. Matter* **7**, 8605 (1995).
26. Y. Xian, in *Condensed Matter Theories*, (eds. M. Casas, M. de Llano, and A. Polls), Nova Science Publ., Commack, New York, 1995, Vol. **10**, p. 541.
27. M. Roger and J.H. Hetherington, *Europhys. Lett.* **11**, 255 (1990); C.F. Lo, E. Manousakis, and Y.L. Wang, *Phys. Lett. A* **156**, 42 (1991); F. Petit and M. Roger, *Phys. Rev. B* **49**, 3453 (1994).
28. C.H. Llewellyn Smith and N.J. Watson, *Phys. Lett. B* **302**, 463 (1993).
29. C. Zeng, D.J.J. Farnell, and R.F. Bishop, UMIST preprint UMIST/Phys/TP/97-2 (1997).
30. T. Barnes, D. Kotchan, and E.S. Swanson, *Phys. Rev. B* **39**, 4357 (1989).
31. K. Kubo and T. Kishi, *Phys. Rev. Lett.* **61**, 2585 (1988).
32. K.J. Runge, *Phys. Rev. B* **45**, 12292 (1992); *ibid.* **45**, 7229 (1992).
33. P.W. Anderson, *Phys. Rev.* **86**, 694 (1952); T. Oguchi, *ibid.* **117**, 117 (1960).
34. R.R.P. Singh, *Phys. Rev. B* **39**, 9760 (1989); R.R.P. Singh and D.A. Huse, *ibid.* **40**, 7247 (1989); W. Zheng, J. Oitmaa, and C.J. Hamer, *ibid.* **43**, 8321 (1991).
35. M. Suzuki, *J. Phys. Soc. Japan* **55**, 4205 (1986).
36. W. Marshall, *Proc. R. Soc. London A* **232**, 48 (1955).
37. M. Boninsegni, *Phys. Rev. B* **52**, 5304 (1995).
38. H. Umezawa, H. Matsumoto, and M. Tachiki, *Thermo Field Dynamics and Condensed States,* North-Holland, Amsterdam, 1982; H. Umezawa and Y. Yamanaka, *Adv. Phys.* **37**, 531 (1988).
39. G. Sanyal, S.H. Mandal, and D. Mukherjee, *Chem. Phys. Lett.* **192**, 55 (1992).